Cherenkov Emission Imaging and Spectroscopy Using a Pulsed Linear Accelerator and the Subsequent Deep-Tissue Imaging of Molecular Oxygen Sensors in a Human Body Phantom

Introduction

Cherenkov radiation, also referred to as either Čerenkov or Cerenkov radiation, takes place when charged particles (e.g., electrons) move through a dielectric (i.e., electrically polarizable) medium at a phase velocity greater than the speed of light in that medium.[1] Emission of this radiation (see Figure 1) occurs as the charged particles lose energy inelastically via electric field interactions with the transiently polarized medium.[2]

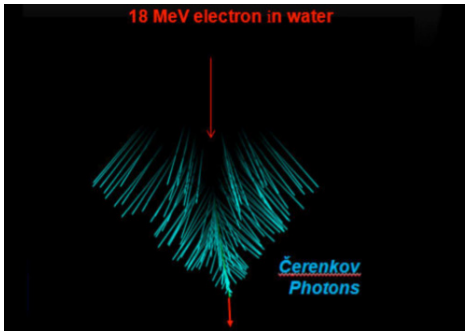

Figure 1.
Cherenkov photons from one electron. Image courtesy of Rongxiao Zhang (Dartmouth College).

As opposed to fluorescence emission spectra, which have characteristic spectral peaks corresponding to quantized energy transitions, Cherenkov radiation is continuous.[3] In the visible portion of the spectrum, its relative intensity per unit frequency is proportional to the frequency (as shown in Figure 2).[4] Thus, because this emission is more intense at higher frequencies (i.e., shorter wavelengths), visible Cherenkov radiation is observed as a brilliant blue.[3] Note that most Cherenkov radiation, however, is actually in the UV portion of the spectrum. Only with sufficiently accelerated charges does it even become visible.

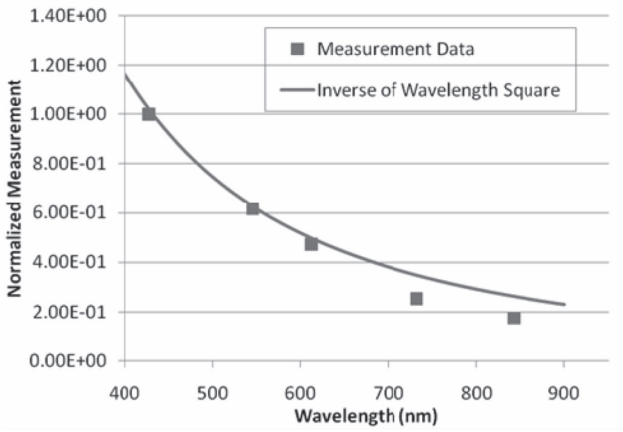

Figure 2.
Results from a series of filtered scans on the wavelength of light detected from positron-emitter samples.[4] The majority of the light is produced in the blue portion of the spectrum, which is expected for Cherenkov radiation, and follows an inverse relationship with the square of the wavelength. Cherenkov light extends into the green and red regions of the EM spectrum, which could increase the range of applications for in vivo imaging studies.

It has been shown that radiation from a linear accelerator, or a LINAC (6 to 24 MeV energy), induces Cherenkov radiation emission in tissue, which produces biochemical spectral signatures — this information can be used to estimate tissue hemoglobin and oxygen saturation or molecular fluorescence from reporters.[5] During radiotherapy, spectral absorption features appearing in the Cherenkov radiation emission spectrum can be utilized to quantify blood oxygen saturation (StO_2) from the known absorptions of hemoglobin.[2]

It has also been demonstrated that isotopic β-emitters (^{18}F, ^{11}C, and ^{13}N, with energy <1 MeV)[3,6,7] generate Cherenkov emission, which is known to be used for optical molecular imaging in small animals.

The most commonly used tracer is the ^{18}F-labeled analog of glucose, 2'-deoxy-2'-[^{18}F]fluoro-D-glucose, or FDG.[4] Metabolically active cells (e.g., in the brain, heart, or malignant tumors) are glucose hungry and therefore accumulate FDG at a higher rate than other tissues.[8] As a marker of cellular glucose consumption and metabolic rate, FDG is employed to assess cancer patients, locate metastatic lesions with higher sensitivity than anatomical imaging modes, and monitor therapeutic response.[9–11]

The Cherenkov visible photon yield with high-energy particles exhibits exponential dependence; its optical emission per particle with a higher-energy beam (i.e., from a LINAC) is approximately 2 to 3 orders of magnitude greater compared to the emission from isotopic β-emitters.[5] Hence, LINAC-based optical molecular imaging is now generating considerable interest for clinical disease treatment and monitoring research, whereas isotopic β-emitters are typically employed for the imaging of small animals (in which far less depth is required).

Clinical Disease Treatment in Human Patients

Until a few years ago, Cherenkov emission spectroscopy (CES) studies had been done with constant wavelength (CW) signal collection in the absence[12,13] of ambient lighting, similar to the isotopic β-emitters–based small-animal imaging method, using conventional CCD or EMCCD detectors — although this technique precluded use on patients owing to the concerns of both patient and physician compliance.[5]

Commercial incandescent lights have an irradiance of 10^{-1} to 10^{-3} W/cm^2, while Cherenkov emission irradiances from a LINAC or a positron emission tomography (PET) agent are approximately 10^{-6} to 10^{-9} W/cm^2 and 10^{-8} to 10^{-12} W/cm^2, respectively, depending directly upon dose rate of irradiation.[5] Such large differences in optical irradiance make CW detection of Cherenkov radiation impossible in the presence of ambient light — PET-agent CES works by imaging in a closed environment with a nearly complete absence of light.[5]

An Important Change in Direction

LINACs employed in radiation oncology can produce radiation in pulsed microseconds-long bursts, generated by the accelerator waveguide.[5] By taking advantage of a LINAC's inherent

pulsed operation, time-gated detection of Cherenkov radiation is possible, significantly improving the ratio of signal to ambient light.[5]

In 2012, a research group at Dartmouth College and Dartmouth-Hitchcock Medical Center in New Hampshire led by Dr. Brian Pogue published results from their investigation into fluorescence and absorption spectroscopy methods using pulsed LINAC-induced CES[2,5] under ambient room lighting conditions.

This application note provides an overview of both that work as well as more recent experiments in which Dr. Pogue and his associates utilized Cherenkov radiation to perform high-resolution luminescence imaging of molecular oxygen sensors located at tissue depths up to 3 cm.

Experimental Setup

In the 2012 Dartmouth studies, optical spectra from a phantom were detected using an imaging spectrograph (a SpectraPro® 300 from Princeton Instruments) equipped with a 300 lines/mm grating blazed at 750 nm and connected to a front-illuminated ICCD camera (a PI-MAX®3:RB from Princeton Instruments) that was configured with a Gen II image intensifier and cooled to −25°C. The optical detection system was placed outside the treatment room and light was collected using a 13 m fiber bundle (Zlight, Latvia) comprising seven 400 µm diameter silica fibers in a hexagonal tip geometry (see Figure 3A).[5]

For each experiment, the fiber tip was placed in the center of the radiation beam at the phantom surface. A trigger-out voltage was obtained from the LINAC control unit and fed into the external trigger port of the ICCD camera using a BNC cable. In an iterative manner, the delay between the falling edge of the trigger signal and the rising edge of the LINAC beam on pulse was found to be 5 µs. The trigger delay, gate width, and frequency were used in conjunction with Princeton Instruments LightField® software to ensure accurate gating and signal acquisition from the spectrometer-ICCD–coupled system (see Figure 3B).[5]

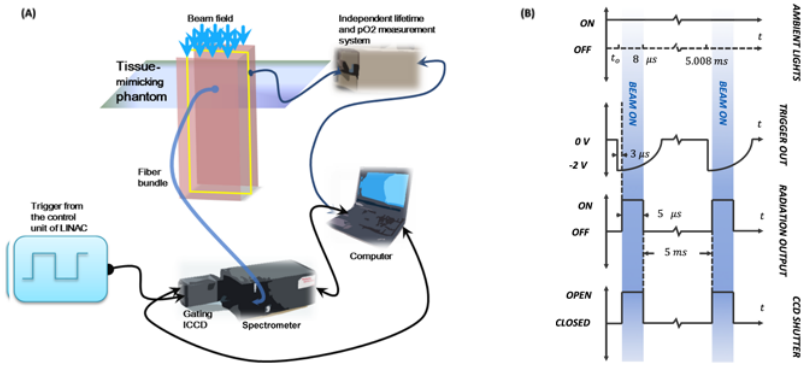

Figure 3.
The geometry of the measurement system and the temporal acquisition process are shown with (A) the fast time-gated spectrometer system[2] as well as (B) the timeline[5] of how the linear accelerator works in pulsed mode and the way to measure decays of Cherenkov radiation emission and excited luminescence (CREL). Diagram and data courtesy of Dr. Brian Pogue (Dartmouth College).

www.princetoninstruments.com | info@princetoninstruments.com
TOLL-FREE +1.877.474.2286 | PHONE +1.609.587.9797
Visit the Princeton Instruments website to find a dealer in your area.

Results

The group explained that the gated signal spectrum was triggered externally by the LINAC with the beam and ambient lights on. Similarly, the ambient lights spectrum was triggered internally with the beam off and gating parameters identical to that of the gated signal. Isolation of the Cherenkov emission signal was obtained by calculating the difference between the two (see Figure 4). All spectra were subject to background subtraction in order to account for characteristic system noise buildup at the high 100/100x gain.[5]

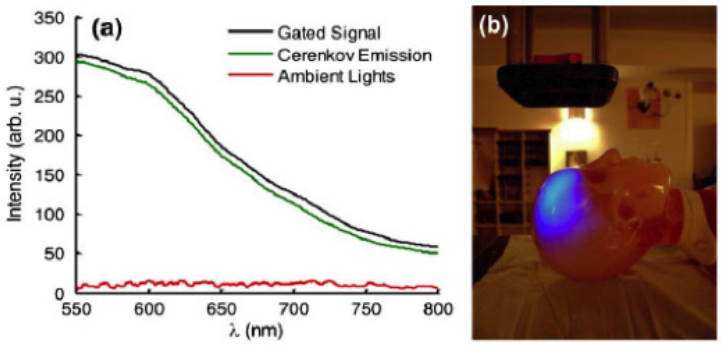

Figure 4.
(a) The gated detection of Cherenkov emission with room lights on is shown with spectra acquired from a scattering phantom. The Cherenkov emission is obtained by calculating the difference between the gated signal and ambient lighting signal.[5] (b) A photograph of the room with a corresponding image of Cherenkov emission from a human head phantom for radiation therapy are overlaid to illustrate the amount of ambient lighting present for all experiments.[5] Data and photograph courtesy of Dr. Brian Pogue (Dartmouth College).

The Dartmouth researchers related that the benefit of such a system can be realized when considering the importance of tumor oxygenation in the outcome of external beam radiotherapy (EBRT), as studies have shown hypoxic tumors to be less responsive to treatment due to inadequate damage to tumor DNA.[14,15] Additional clinical studies have also correlated tissue oxygen pressure (pO2) to EBRT effect in head and neck cancers and suggested that pO2 increases during fractionated treatment plans.[16,17] Therefore, there is great potential value in a noninvasive technique, such as CES, for monitoring tumor oxygen saturation during EBRT.[5]

The group emphasized that the inability to make measurements in a conventional radiation treatment environment where ambient room light is always present raises significant concern for patient and physician compliance; however, the gated ICCD camera system they presented offers a better solution to this problem via ~1000x reduction in ambient light contribution to the CES signal when the radiation is gated, such as with a LINAC.[5]

It is worth noting that because small-animal imaging can be conducted in a dark environment (i.e., with a dark box) and utilizes isotopic β-emitters, which inherently have 2 to 3 orders of magnitude less visible light yield, a higher-sensitivity, electron-multiplying ICCD (*em*ICCD) camera such as the Princeton Instruments PI-MAX4:512EM* can be utilized instead of a traditional ICCD camera.

www.princetoninstruments.com | info@princetoninstruments.com
TOLL-FREE +1.877.474.2286 | PHONE +1.609.587.9797
Visit the Princeton Instruments website to find a dealer in your area.

New Studies

More recently, Dr. Pogue and several of his associates utilized Cherenkov-excited luminescence scanned imaging (CELSI) in a human body geometry to demonstrate the capability of imaging local oxygenation in regions similar in size to lymph nodes (see Figure 5). The effects of depth, concentration, and minimum radiation dose were examined.[20]

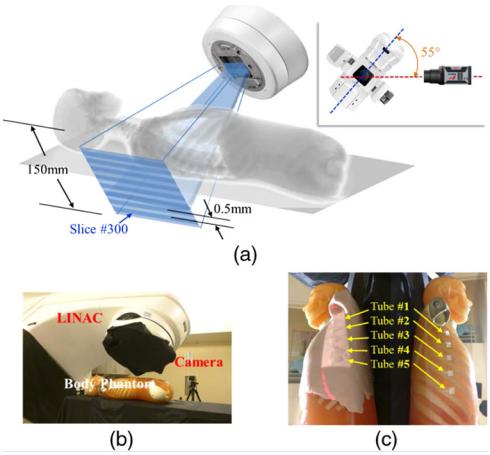

Figure 5.
Measurement geometry for the body phantom is shown with (a) a schematic of the geometry, (b) a photograph of the setup, and (c) the body phantom with skin on (left) and without skin (right) with five tubes fixed onto the lateral rib area.[20] Diagrams and photographs courtesy of Dr. Brian Pogue, Dartmouth College; first published in J. Biomed. Opt. 23 (3), 030504 (2018), doi: 10.1117/1.JBO.23.3.030504.

The CELSI technique employed by the researchers uses sheet-shaped radiation beams from a LINAC to produce Cherenkov photons. These photons excite probe luminescence in a volume confined primarily to the irradiation sheets. By shaping the x-ray beam into a thin sheet, images of Cherenkov-excited luminescence from a planar slice within the tissue can be acquired. A series of luminescence images is taken at different depths, thus providing a three-dimensional volumetric rendering.[20]

A Princeton Instruments PI-MAX4:1024i* gated ICCD camera with LightField software was employed for image acquisition (see Figure 6). The researchers note that an epi-illumination configuration was used, with the LINAC gantry oriented at 145 degrees and on the same side as the camera. The ICCD gate delays and widths were adjusted in the following manner: a 0.05 µs delay and 4 µs width for Cherenkov imaging; a 4.2 µs delay and 70 µs width for phosphorescence imaging; and a 1500 µs delay and 70 µs width for background imaging. All images were acquired using a 100x intensifier gain. The camera system's Gen III image intensifier was gated by a predefined number of pulses, whereas the CCD integrated the signal prior to readout.[20]

Figure 6.
PI-MAX4:1024i-HR gated ICCD camera from Princeton Instruments.

Different values of this approach to accumulations on the chip, or AoC, were utilized in each of the Cherenkov, phosphorescence, and background images for all experiments performed. Room-light images were collected using 1x gain and 1 AoC. An 8 MHz analog-to-digital conversion rate was used with 2 x 2 pixel hardware binning upon readout, yielding 512 x 512 pixel images.[20]

In the depth and concentration ranging studies, CELSI experiments were performed for an intralipid-blood phantom embedded with PtG4-containing 0.5 mm Eppendorf tubes. Results are presented in Figure 7. To pursue a minimum radiation dose, sparse illumination was also investigated.[20]

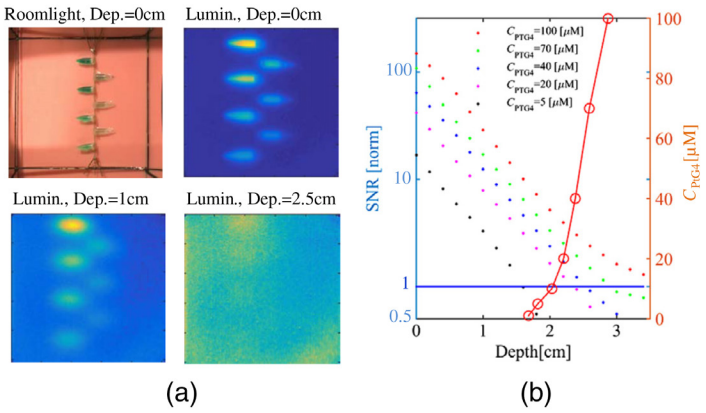

Figure 7.
Image quality vs. depth for different concentrations of PtG4 (C_{PtG4}) as depicted in the legend, showing (a) the room-light image and luminescence images of the phantom at three different depths in the phantom, and (b) the corresponding signal-to-noise ratio extracted from these images as a function of depth (colored dots). In the same graph, the red line shows the C_{PtG4} at which SNR = 1 (values on left y-axis).[20] Data courtesy of Dr. Brian Pogue, Dartmouth College; first published in J. Biomed. Opt. 23 (3), 030504 (2018), doi: 10.1117/1. JBO.23.3.030504.

The researchers explain that initial studies of depth sensitivity have indicated CELSI would be viable for a depth of 2 to 3 cm, depending on tissue type, and that the focus of their own study was to determine the optimal positioning of the body phantom, couch, gantry, and camera in order to achieve maximum sensitivity. This investigation shows that sensing the oxygenation of lymph-node–sized objects via CELSI is feasible, and further exploration of agents and signal analysis could lead to the next clinical trials in molecular sensing in radiotherapy.[20]

In another recently published study, Dr. Pogue and associates report on their use of CELSI both in live mice and in tissue phantoms. Once again, a PI-MAX4:1024i gated ICCD camera from Princeton Instruments was utilized for the experiments, which demonstrate *in vivo* mapping of the oxygenation of tumors at depths of several millimeters, with submillimeter resolution and nanomolar sensitivity.[21]

By employing phantoms and simulations, the researchers show the performance of CELSI is limited by beam size, scan geometry, probe concentration, radiation dose, and tissue depth. They conclude that CELSI might provide the highest sensitivity and resolution in the optical imaging of molecular tracers *in vivo*.[21]

www.princetoninstruments.com | info@princetoninstruments.com
TOLL-FREE +1.877.474.2286 | PHONE +1.609.587.9797
Visit the Princeton Instruments website to find a dealer in your area.

For more data and a comprehensive discussion of recent work, please read:

Syed Rakin Ahmed, Jeremy Mengyu Jia, Petr Bruza, Sergei Vinogradov, Shudong Jiang, David J. Gladstone, Lesley A. Jarvis, Brian W. Pogue, "Radiotherapy-induced Cherenkov luminescence imaging in a human body phantom," *J. Biomed. Opt.* 23 (3), 030504 (2018), doi: 10.1117/1.JBO.23.3.030504.

Brian W. Pogue, Jinchao Feng, Ethan P. LaRochelle, Petr Bruža, Huiyun Lin, Rongxiao Zhang, Jennifer R. Shell, Hamid Dehghani, Scott C. Davis, Sergei A. Vinogradov, David J. Gladstone, and Lesley A. Jarvis, "Maps of *in vivo* oxygen pressure with submillimetre resolution and nanomolar sensitivity enabled by Cherenkov-excited luminescence scanned imaging," *Nat. Biomed. Eng.* 2, pp. 254–264 (2018), https://doi.org/10.1038/s41551-018-0220-3.

Resources

To learn more about Dr. Pogue's research at Dartmouth, please visit:
http://engineering.dartmouth.edu/people/faculty/brian-pogue/

For additional information about Princeton Instruments ICCD and *em*ICCD cameras, please visit: **http://www.pi-max4.com**

References

1. P.A. Cherenkov, *C.R. Acad. Sci. URSS* 20, 651–655 (1938).

2. R. Zhang, A. Glaser, T.V. Esipova, S.C. Kanick, S.C. Davis, S. Vinogradov, D. Gladstone, and B. Pogue, *Biomed. Opt. Express.* 3(10), 2381–2394 (2012).

3. J.V. Jelley, Br. *J. Appl. Phys.* 6(7), 227–232 (1955).

4. R. Robertson, M.S. Germanos, C. Li, G.S. Mitchell, S.R. Cherry, and M.D. Silva, *Phys. Med. Biol.* 54, N355 (2009). [Author manuscript cited; available via NIH Public Access.]

5. A.K. Glaser, R. Zhang, S.C. Davis, D.J. Gladstone, and B.W. Pogue, *Opt. Lett.* 37(7), 1193–1195 (2012).

6. S.M. Ametamey, M. Honer, and P.A. Schubiger, *Chem. Rev.* 108, 1501–1516 (2008).

7. H.H. Ross, *Anal. Chem.* 41, 1260–1265 (1969).

8. O. Warburg, *Science* 123, 309–314 (1956). [PubMed: 13298683]

9. G.J. Kelloff, J.M. Hoffman, B. Johnson, H.I. Scher, B.A. Siegel, E.Y. Cheng, B.D. Cheson, J. O'Shaughnessy, K.Z. Guyton, M.A. Mankoff, L. Shankar, S.M. Larson, C.C. Sigman, R.L. Schilsky, and D.C. Sullivan, *Clin. Cancer Res.* 11, 2785–2808 (2005). [PubMed: 15837727]

10. N.G. Mikhaeel, M. Hutchings, P.A. Fields, M.J. O'Doherty, and A.R. Timothy, *Ann. Oncol.* 16, 1514–1523 (2005). [PubMed: 15980161]

11. L.K. Shankar, J.M. Hoffman, S. Bacharach, M.M. Graham, J. Karp, A.A. Lammertsma, S. Larson, D.A. Mankoff, B.A. Siegel, A. Van den Abbeele, J. Yap, and D. Sullivan, *J. Nucl. Med.* 47, 1059–1066 (2006). [PubMed: 16741317]

12. J. Axelsson, S.C. Davis, D.J. Gladstone, and B.W. Pogue, *Med. Phys.* 38(7), 4127 (2011).

13. J. Axelsson, A.K. Glaser, D.J. Gladstone, and B.W. Pogue, *Opt. Express* 20, 5133 (2012).

14. P. Vaupel, A. Mayer, and M. Höckel in Recombinant Human Erythropoietin (rhEPO) in *Clinical Oncology,* M.R. Nowrousian, eds. (Springer, 2008) pp. 265–282.

15. S.M. Evans and C.J. Koch, *Cancer Lett.* 195, 1 (2003).

16. M. Nordsmark, S.M. Bentzen, V. Rudat, D. Brizel, E. Lartigau, P. Stadler, A. Becker, M. Adam, M. Molls, J. Dunst, D.J. Terris, and J. Overgaard, *Radiother. Oncol.* 77, 18 (2005).

17. R.A. Cooper, C.M. West, J.P. Logue, S.E. Davidson, A. Miller, S. Roberts, I.J. Statford, D.J. Honess, and R.D. Hunter, *Int. J. Radiat. Oncol. Biol. Phys.* 45, 119 (1999).

18. R. Zhang, D.J. Gladstone, L.A. Jarvis, R.R. Strawbridge, P. Jack Hoopes, O.D. Friedman, A.K. Glaser, and B.W. Pogue, "Real-time in vivo Cherenkoscopy imaging during external beam radiation therapy," *J. Biomed. Opt.* 2013 Nov; 18(11): 110504.

19. Lesley A. Jarvis, Rongxiao Zhang, David J. Gladstone, Shudong Jiang, Whitney Hitchcock, Oscar D. Friedman, Adam K. Glaser, Michael Jermyn, and Brian W. Pogue, "Cherenkov video imaging allows for the first visualization of radiation therapy in real time," *Int. J. Radiation Oncology, Biology & Physics* 89 (3), pp. 623–625 (2014), doi: 10.1016/j.ijrobp.2014.01.046.

20. Syed Rakin Ahmed, Jeremy Mengyu Jia, Petr Bruza, Sergei Vinogradov, Shudong Jiang, David J. Gladstone, Lesley A. Jarvis, and Brian W. Pogue, "Radiotherapy-induced Cherenkov luminescence imaging in a human body phantom," *J. Biomed. Opt.* 23 (3), 030504 (2018), doi: 10.1117/1.JBO.23.3.030504.

21. Brian W. Pogue, Jinchao Feng, Ethan P. LaRochelle, Petr Bruža, Huiyun Lin, Rongxiao Zhang, Jennifer R. Shell, Hamid Dehghani, Scott C. Davis, Sergei A. Vinogradov, David J. Gladstone, and Lesley A. Jarvis, "Maps of *in vivo* oxygen pressure with submillimetre resolution and nanomolar sensitivity enabled by Cherenkov-excited luminescence scanned imaging," *Nat. Biomed. Eng.* 2, pp. 254–264 (2018), https://doi.org/10.1038/s41551-018-0220-3.

** Please note that all PI-MAX4 cameras with a Gen III image intensifier or an EMCCD require an end-user statement and licensing process for shipments outside the United States.*